

## Synthesis and characterization of MgZnCo ternary mixed metal oxide by the sonochemical method for solid hydrogen storage

Safia HARRAT <sup>1,\*</sup>, Mounir SAHLI <sup>1</sup>, Abdelhakim SETTAR <sup>2</sup>, Khaled CHETHOUNA <sup>2</sup>

<sup>1</sup> Université Frère Mentouri Constantine 1, Ceramics laboratory Constantine - Algeria

<sup>2</sup> INSA Centre Val de Loir, PRISM laboratory EA 18000 Bourges – France

\*Corresponding author: [safia.harrat@student.umc.edu.dz](mailto:safia.harrat@student.umc.edu.dz)

**Abstract** – In the present investigation, MgZnCo ternary nanocomposites were developed via a one-step sonochemical technique. The nanocomposite was characterized using structural and optical methods. The formation of different crystalline nanocomposite phases (MgO, ZnO, and Co<sub>3</sub>O<sub>4</sub>), and a binary phase (Mg-Zn) has been confirmed by X-ray diffraction. Also, it was indicated that varying of Co molar ratio had an impact on the average sizes of the nanoparticles. SEM showed octahedron-shaped nanoparticle morphology with different average sizes for the nanocomposites prepared. Photoluminescence analysis showed the presence of green and ultraviolet emissions, with green luminescence bands being most often observed. with the intention of discovering samples with suitable structural and optical properties for future solid hydrogen storage applications.

**Keywords** – Nanostucture, Ternary Nanocomposites, Morphology, Hydrogen Storage.

### 1. Introduction

Magnesium oxide (MgO), Zinc oxide (ZnO), and cobalt oxide (Co<sub>3</sub>O<sub>4</sub>) are the three vital TMOs widely reported for a variety of applications such as photocatalysis, biosensors, batteries, solar cells, supercapacitors, hydrogen storage, etc. Owing to their physiochemical and electrocatalytic properties such as the higher surface to volume ratio, chemical stability, structural properties, non-toxicity, etc. [1-

2-3]. In most studies, the synthesis of this complexes were reported via Sol-gel method, co-precipitation method, and the hydrothermal method [1-4-5]. These conventional techniques typically necessitate prolonged exposure to high pressure or temperatures, which can be challenging. Fortunately, the utilization of sonochemistry can provide a solution to these issues, the utilization of this approach has gained significant importance as a

means to achieve consistent size and morphology for a variety of nanostructures during synthesis [6]. In storage application, storage of hydrogen in metal hydrides, emerges as a prospective approach for addressing the problems of hydrogen storage [7]. As supported by previous studies, structural properties, including grain size, can affect the storage capacity of hydrogen, with small grains having better absorption and desorption of hydrogen than large ones [8-9].

This research focused on synthesis of ternary metal oxide nanocomposites based on Mg, Zn and Co by the sonochemical method, and investigating the effect of Co molar ratio on the phase composition and morphology of this compound. for achieving enhanced hydrogen storage structural and optical properties and elucidating the underlying mechanisms responsible for the observed changes.

## 2. Synthesis method

In this study, a one-pot synthesis of Mg-Zn-Co ternary was conducted using the sonochemical method. Magnesium chloride ( $\text{MgCl}_2 \cdot 6\text{H}_2\text{O}$ ), zinc chloride ( $\text{ZnCl}_2$ ), and cobalt (II) chloride hexahydrate ( $\text{CoCl}_2 \cdot 6\text{H}_2\text{O}$ ) were utilized as the starting materials in molar ratio of 1:1:1. These were dispersed in deionized water, and the mixture is stirred by a magnetic stirrer for 30 min under a temperature of 60 °C. To complete the reaction mechanism, the solution is sonicated for 15 min at 20 kHz of frequency and 1500 W, and the mixture

is dried for 48 h of 110 °C of temperature to form a powder and to remove water molecules. Finally, the dried powder is calcinated for 2 h in a muffle furnace at 550 °C to obtain the desired Mg-Zn-Co nanocomposite oxide powder. Following the same experimental protocol for S2 and S3, with molar ratios of 1:1:2 and 1:1:3, respectively.

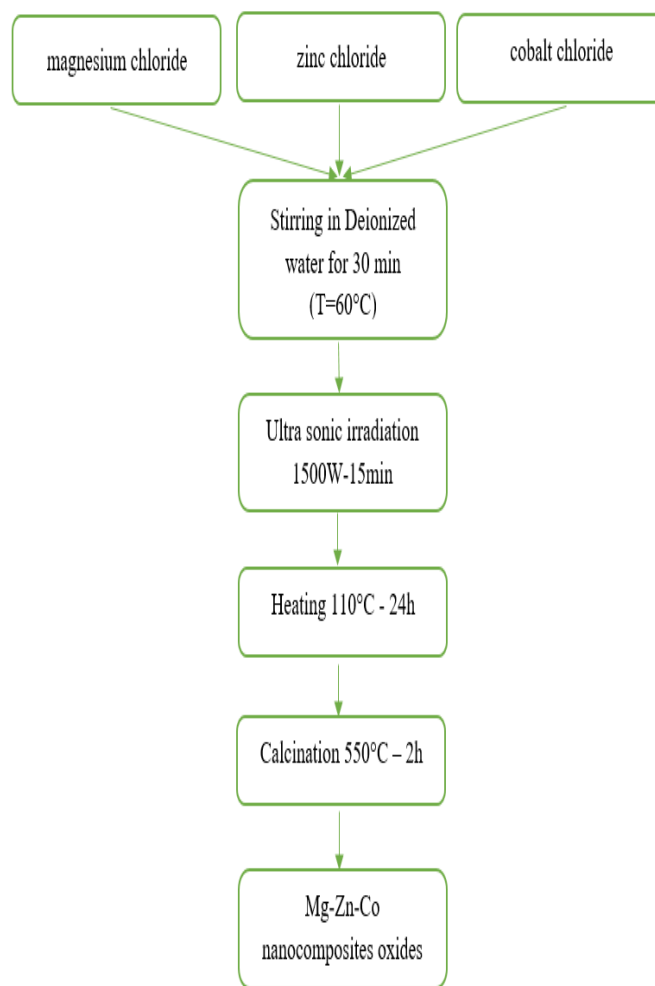


Figure 1. Process diagram for Mg-Zn-Co nanoparticle oxide synthesis by the sonochemical method

### 3. Results and discussion

#### 3.1 XRD Results

Figure 2 shows the X-ray diffraction (XRD) spectra of the prepared nanocomposites containing Mg, Zn, and Co. The XRD analysis aims to control the characteristics of crystallography and to obtain the final composition of the studied nanocomposites. XRD spectra depict several peaks indicating the evidence of multiphase structure. The XRD results reveal mainly two multiphase structures: (1) three metal-oxide structures (MgO, ZnO and  $\text{Co}_3\text{O}_4$ ) and (2) one binary structure (Mg-Zn). Peaks at  $2\theta = 37.2^\circ$ ,  $43.2^\circ$ ,  $62.4^\circ$ , and  $78.8^\circ$  are attributed to a single-phase cubic system of MgO, corresponding respectively to the (111), (200), (220), and (222) plans (JCPDS database card number 75-1525).

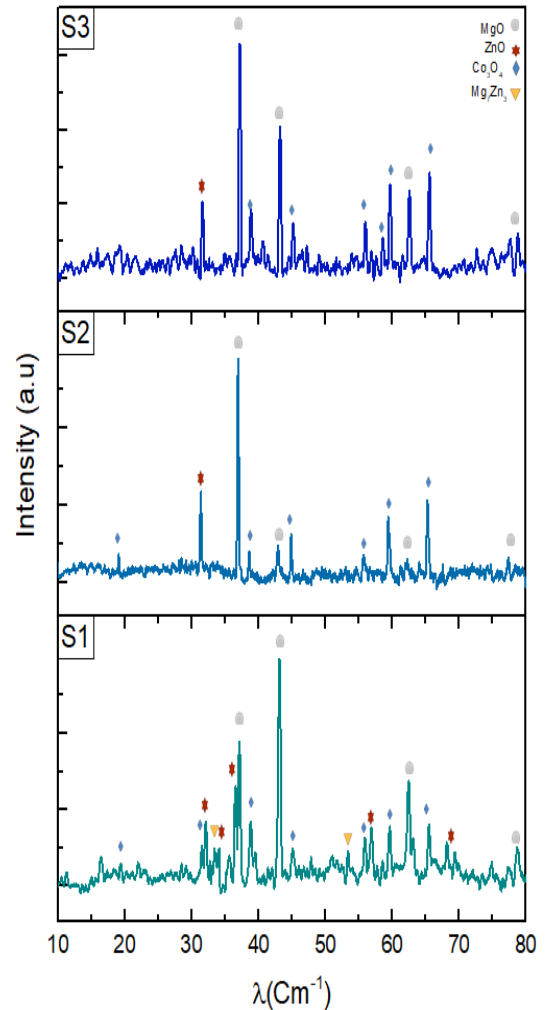


Figure 2. XRD graphs for the investigated nanocomposite samples.

Furthermore, the XRD pattern reveals the presence of ZnO nanoparticles belonging to the hexagonal wurtzite structure at  $2\theta = 31.5^\circ$ ,  $34.7^\circ$ ,  $36.6^\circ$ ,  $56.9^\circ$ , and  $68.2^\circ$ , which correspond to the plans (100), (002), (101), (110), and (112), respectively (JCPDS database card numbers 75-1526 and 74-0534). For the  $\text{Co}_3\text{O}_4$  structure (cubic), it is identified by peaks appearing at  $2\theta = 19.1^\circ$ ,  $31.4^\circ$ ,  $38.8^\circ$ ,  $45.1^\circ$ ,  $55.9^\circ$ ,  $59.6^\circ$ , and  $65.4^\circ$  which are indexed to the plans (111), (220), (222), (400), (422), (511) and (440),

respectively (JCPDS database card numbers 74-1656 and 80-1537). Concerning the metal-metal structure (Mg-Zn),  $Mg_7Zn_3$  phase is detected at  $2\theta = 33.4^\circ$  and  $51.8^\circ$  which are indexed to the plans (521) and (800) respectively (JCPDS database card number 08-0269).

The crystallite size of Mg-Zn-Co nanocomposites oxide was determined by using the Scherer equation (1) given below [10]:

$$D = \frac{K\lambda}{\beta \cos\theta} \quad (1)$$

Where D is the crystallite size, K is a dimensionless shape factor (0.9),  $\lambda$  is the X-ray wavelength (1.5406),  $\theta$  is the Bragg angle, and  $\beta$  is the full width at half maximum intensity (FWHM).

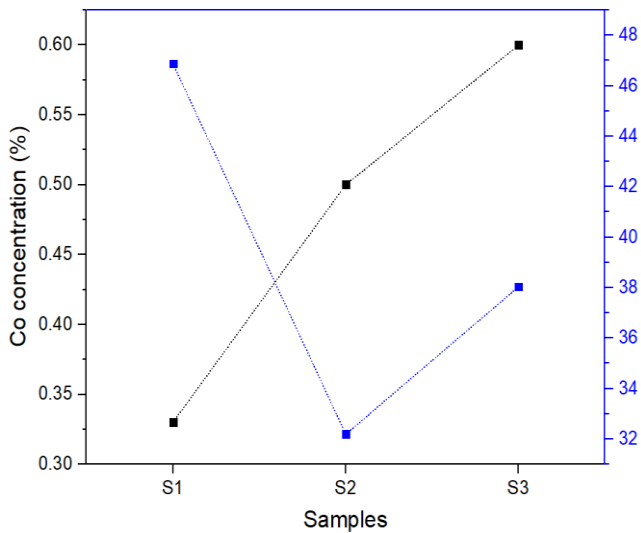


Figure 3. Grain size variation as function of Co concentration.

Experimental observations, indicate that an increase in the number of cobalt moles in the solution

resulted in a significant reduction in the grain size of the granules compared to the initial sample, which contained an equal amount of materials (Mg-Zn-Co), 1:1:1. This phenomenon can be attributed to grain boundary pinning, a widely recognized mechanism for grain refinement. Grain boundary pinning involves introducing of grains, resulting in smaller grain sizes [11-12]. In the present work, the addition of Co to Mg-Zn induces a substantial grain refinement effect, where the average grain size decreases as the cobalt content increases [13]. The hydrogen storage properties discovered in research that with small grains have a better absorption and desorption of hydrogen than large ones.

### 3.2. SEM analysis

SEM micrographs for the ternary samples are given by Figure 4. The micrographs show two different shapes, octahedral and spherical shapes, with octahedral shape dominance. The octahedral shape is formed by the arrangement of metal and oxygen atoms in specific way. There are six oxygen atoms located at the corners of an octahedron, and a metal atom at the center of the octahedron [14]. The appearance of this morphology is explained by the fact that the two dominating crystal structure in samples are  $Co_3O_4$  and  $MgO$  [15-16], which have the highest molar fraction comparing to  $ZnO$  phase. It is also promoted when the starting solution pH is low, which is the case for all synthesised samples [17]. The observed particles were conglomerated,

hindering of their relative size, this is attributed to nucleation and crystal growth phenomena occurring during thermal processing [18]. It is hypothesized that the reaction temperature during the onset of nucleation governs the resulting particle size.

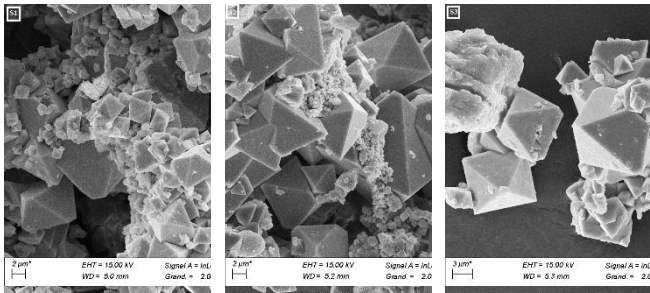


Figure 4. SEM images for the studied nanocomposite samples

The EDS results are depicted in Figure 5 which demonstrate the atomic % values of Mg, Zn, Co and O Elements. The results show that the Zn % is very low compared to those of cobalt, implying that Co exhibits a more favorable diffusion behavior.

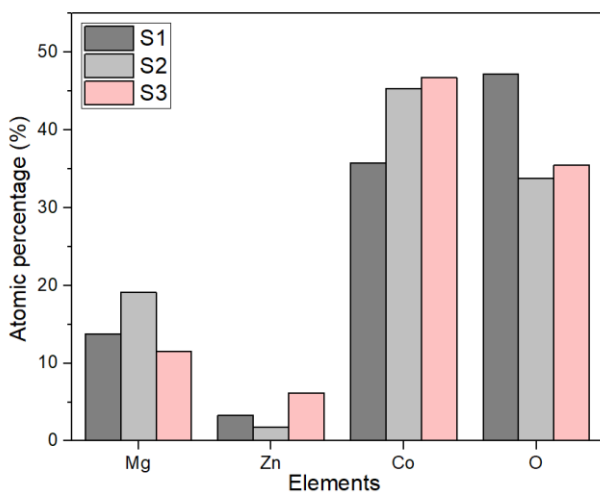


Figure 5. EDS results for the studied nanocomposite samples

### 3.3. Photoluminescence spectroscopy analysis

The photoluminescence of ternary nanocomposites samples was exhibited in Figure 5, with an excitation wavelength of 325 nm. The emission spectra reveal a different luminescence performance from one sample to another. The PL spectrum of the reference S1, presents two emission bands. The first is around 388 nm, which is attributed to excitation emission between an electron close to the conduction band and a hole in the valence band (ultraviolet emission). The second is a large band of high intensity that included to the green, is located at 510 nm. The green luminescence band is related to oxygen vacancies.[19]

It can be observed that the UV and barycenter (Green) emissions are shifted from 388 to 414 nm which contains more Co ions.

Also, as S2 and S3 with high molar fraction of cobalt show the green emission at 554 nm for S4, shifted at 584 for S5 related to  $O^{2-} \rightarrow Co^{3+}$  charge transfer [20]. And the peaks located at around 600 nm correspond to the yellow emission [21].

In the photoluminescence spectra of the samples, it is discovered that nanostructure defects considerably contribute to the studied green emission bands. The hydrogen storage properties discovered in research show that higher hydrogen absorption is caused by nanostructures defects [22].

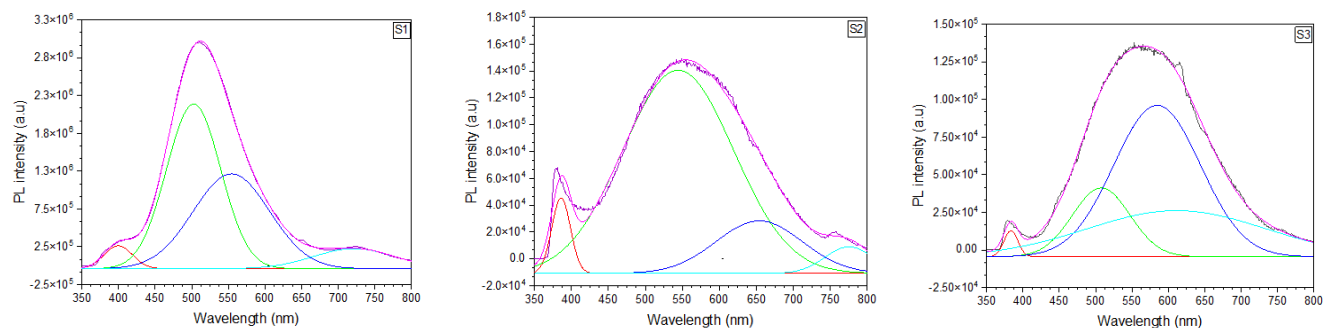


Figure 5. Photoluminescence spectra of the studied nanocomposite samples

#### 4. Conclusion

The objectives of this work are twofold. Firstly, to synthesize MgZnCo ternary mixed metal oxide using the sonochemical method. And secondly, to investigate the impact of Co molar ratio on the properties of the samples and determine their optimal structural and optical properties of solid hydrogen storage. The nanocomposites obtained were characterized using: XRD diffraction confirmed that the samples had a complex crystalline structure consisting of various crystalline phases of different compositions, including MgO, Co<sub>3</sub>O<sub>4</sub>, ZnO, and Mg-Zn phases. Also, it was indicated that varying of Co molar ratio had an impact on the average sizes of the nanoparticles. SEM micrographs showed the octahedron shape morphology of the samples with different average size. The photoluminescence analysis included the optical information about the synthesised samples such as; energy levels and defect states. The results show the green, and ultra violet emission. In which, the green luminescence bands were most often observed compared to the others. Based on the

results obtained from this study, it can be concluded that certain samples (S2, and S3), in terms of their structure, morphology, and optical properties, exhibit promising potential for hydrogen storage applications.

#### References

- [1] L. Durai, A. Gopalakrishnan, and S. Badhulika, "One-pot hydrothermal synthesis of NiCoZn a ternary mixed metal oxide nanorod based electrochemical sensor for trace level recognition of dopamine in biofluids," *Materials Letters*, vol. 298, p. 130044, Sep. 2021, doi: 10.1016/j.matlet.2021.130044.
- [2] A. Sulciute *et al.*, "ZnO Nanostructures Application in Electrochemistry: Influence of Morphology," *J. Phys. Chem. C*, vol. 125, no. 2, pp. 1472–1482, Jan. 2021, doi: 10.1021/acs.jpcc.0c08459.
- [3] J. P. Mojica-Sánchez, T. I. Zarate-López, J. M. Flores-Álvarez, J. Reyes-Gómez, K. Pineda-Urbina, and Z. Gómez-Sandoval, "Magnesium oxide clusters as promising candidates for hydrogen storage," *Phys. Chem. Chem. Phys.*, vol. 21, no. 41, pp. 23102–23110, 2019, doi: 10.1039/C9CP05075B.
- [4] K. Jung, "Local structure and photocatalytic activity of B<sub>2</sub>O<sub>3</sub>-SiO<sub>2</sub>/TiO<sub>2</sub> ternary mixed oxides prepared by sol-gel method," *Applied Catalysis B: Environmental*, vol. 51, no. 4, pp. 239–245, Aug. 2004, doi: 10.1016/j.apcatb.2004.03.010.
- [5] Y. I. Kim, D. Kim, and C. S. Lee, "Synthesis and characterization of CoFe<sub>2</sub>O<sub>4</sub> magnetic nanoparticles prepared by temperature-controlled coprecipitation method," *Physica B: Condensed Matter*, vol. 337, no. 1–4, pp. 42–51, Sep. 2003, doi: 10.1016/S0921-4526(03)00322-3.
- [6] M. Masjedi-Arani, M. Salavati-Niasari, D. Ghanbari, and G. Nabilyouni, "A sonochemical-assisted synthesis of spherical silica nanostructures by using a new capping

- agent,” *Ceramics International*, vol. 40, no. 1, pp. 495–499, Jan. 2014, doi: 10.1016/j.ceramint.2013.06.029.
- [7] S.-Y. Lee, J.-H. Lee, Y.-H. Kim, J.-W. Kim, K.-J. Lee, and S.-J. Park, “Recent Progress Using Solid-State Materials for Hydrogen Storage: A Short Review,” *Processes*, vol. 10, no. 2, Art. no. 2, Feb. 2022, doi: 10.3390/pr10020304.
- [8] V. Bérubé, G. Radtke, M. Dresselhaus, and G. Chen, “Size effects on the hydrogen storage properties of nanostructured metal hydrides: A review,” *Int. J. Energy Res.*, vol. 31, no. 6–7, pp. 637–663, May 2007, doi: 10.1002/er.1284.
- [9] T. Gholami, M. Salavati-Niasari, and S. Varshoy, “Electrochemical hydrogen storage capacity and optical properties of NiAl<sub>2</sub>O<sub>4</sub>/NiO nanocomposite synthesized by green method,” *International Journal of Hydrogen Energy*, vol. 42, no. 8, pp. 5235–5245, Feb. 2017, doi: 10.1016/j.ijhydene.2016.10.132.
- [10] S. Fatimah, R. Ragadhita, D. F. A. Husaeni, and A. B. D. Nandiyanto, “How to Calculate Crystallite Size from X-Ray Diffraction (XRD) using Scherrer Method,” *ASEAN J. Sci. Eng.*, vol. 2, no. 1, pp. 65–76, Jun. 2021, doi: 10.17509/ajse.v2i1.37647.
- [11] R. Z. Valiev and T. G. Langdon, “Principles of equal-channel angular pressing as a processing tool for grain refinement,” *Progress in Materials Science*, vol. 51, no. 7, pp. 881–981, Sep. 2006, doi: 10.1016/j.pmatsci.2006.02.003.
- [12] T. G. Langdon, “The principles of grain refinement in equal-channel angular pressing,” *Materials Science and Engineering: A*, vol. 462, no. 1–2, pp. 3–11, Jul. 2007, doi: 10.1016/j.msea.2006.02.473.
- [13] M. Golrang, M. Mobasheri, H. Mirzadeh, and M. Emany, “Effect of Zn addition on the microstructure and mechanical properties of Mg-0.5Ca-0.5RE magnesium alloy,” *Journal of Alloys and Compounds*, vol. 815, p. 152380, Jan. 2020, doi: 10.1016/j.jallcom.2019.152380.
- [14] W. Zhang *et al.*, “Magnetic transformation of Zn-substituted Mg-Co ferrite nanoparticles: Hard magnetism → soft magnetism,” *Journal of Magnetism and Magnetic Materials*, vol. 506, p. 166623, Jul. 2020, doi: 10.1016/j.jmmm.2020.166623.
- [15] S. S. Sainudeen, L. B. Asok, A. Varghese, A. S. Nair, and G. Krishnan, “Surfactant-driven direct synthesis of a hierarchical hollow MgO nanofiber–nanoparticle composite by electrospinning,” *RSC Adv.*, vol. 7, no. 56, pp. 35160–35168, 2017, doi: 10.1039/C7RA05812H.
- [16] E. U. Ikhuoria, S. O. Omorogbe, B. T. Sone, and M. Maaza, “Bioinspired shape controlled antiferromagnetic Co<sub>3</sub>O<sub>4</sub> with prism like-anchored octahedron morphology: A facile green synthesis using Manihot esculenta Crantz extract,” *Science and Technology of Materials*, vol. 30, no. 2, pp. 92–98, May 2018, doi: 10.1016/j.stmat.2018.02.003.
- [17] X. Xiao *et al.*, “Facile Shape Control of Co<sub>3</sub>O<sub>4</sub> and the Effect of the Crystal Plane on Electrochemical Performance,” *Adv. Mater.*, vol. 24, no. 42, pp. 5762–5766, Nov. 2012, doi: 10.1002/adma.201202271.
- [18] R. K. Gupta, A. K. Sinha, B. N. Raja Sekhar, A. K. Srivastava, G. Singh, and S. K. Deb, “Synthesis and characterization of various phases of cobalt oxide nanoparticles using inorganic precursor,” *Appl. Phys. A*, vol. 103, no. 1, pp. 13–19, Apr. 2011, doi: 10.1007/s00339-011-6311-6.
- [19] S. R. *et al.*, “Excellent Photocatalytic degradation of Methylene Blue, Rhodamine B and Methyl Orange dyes by Ag-ZnO nanocomposite under natural sunlight irradiation,” *Optik*, vol. 231, p. 166518, Apr. 2021, doi: 10.1016/j.ijleo.2021.166518.
- [20] G. Anandha Babu, G. Ravi, Y. Hayakawa, and M. Kumaresavanji, “Synthesis and calcinations effects on size analysis of Co<sub>3</sub>O<sub>4</sub> nanospheres and their superparamagnetic behaviors,” *Journal of Magnetism and Magnetic Materials*, vol. 375, pp. 184–193, Feb. 2015, doi: 10.1016/j.jmmm.2014.09.062.
- [21] S. Li, X. Zhang, B. Yan, and T. Yu, “Growth mechanism and diameter control of well-aligned small-diameter ZnO nanowire arrays synthesized by a catalyst-free thermal evaporation method,” *Nanotechnology*, vol. 20, no. 49, p. 495604, Dec. 2009, doi: 10.1088/0957-4484/20/49/495604.
- [22] M. Ahmad, Rafi-ud-Din, C. Pan, and J. Zhu, “Investigation of Hydrogen Storage Capabilities of ZnO-Based Nanostructures,” *J. Phys. Chem. C*, vol. 114, no. 6, pp. 2560–2565, Feb. 2010, doi: 10.1021/jp100037u.